

Maitree Biswas,^a Susmita
Khamrui,^{b,‡} Udayaditya Sen^b and
Jhimli Dasgupta^{a*}^aDepartment of Biotechnology, St Xavier's
College, 30 Park Street, Kolkata 700 016, India,
and ^bCrystallography and Molecular Biology
Division, Saha Institute of Nuclear Physics,
1/AF Bidhannagar, Kolkata 700 064, India‡ Current address: Department of Biochemistry,
University of Washington, Seattle, Washington,
USA.Correspondence e-mail:
jhimlidasgupta@yahoo.com

Received 18 August 2011

Accepted 11 October 2011

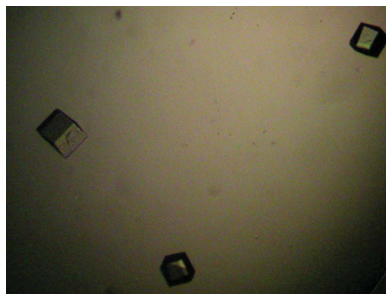
Overexpression, purification, crystallization and preliminary X-ray analysis of CheY4 from *Vibrio cholerae* O395

Chemotaxis and motility greatly influence the infectivity of *Vibrio cholerae*, although the role of chemotaxis genes in *V. cholerae* pathogenesis is poorly understood. In contrast to the single copy of CheY found in *Escherichia coli* and *Salmonella typhimurium*, four CheYs (CheY1–CheY4) are present in *V. cholerae*. While insertional disruption of the *cheY4* gene results in decreased motility, insertional duplication of this gene increases motility and causes enhanced expression of the two major virulence genes. Additionally, *cheY3/cheY4* influences the activation of the transcription factor NF- κ B, which triggers the generation of acute inflammatory responses. *V. cholerae* CheY4 was cloned, overexpressed and purified by Ni-NTA affinity chromatography followed by gel filtration. Crystals of CheY4 grown in space group C2 diffracted to 1.67 Å resolution, with unit-cell parameters $a = 94.4$, $b = 31.9$, $c = 32.6$ Å, $\beta = 96.5^\circ$, whereas crystals grown in space group P3₂21 diffracted to 1.9 Å resolution, with unit-cell parameters $a = b = 56.104$, $c = 72.283$ Å, $\gamma = 120^\circ$.

1. Introduction

Vibrio cholerae, the aetiological agent of cholera, colonizes the small intestine, produces enterotoxin and causes an acute inflammatory response at the intestinal epithelial surface (Butler & Camilli, 2004). This highly motile organism uses the processes of motility and chemotaxis to travel from the lumen of the small intestine to its preferred intestinal niche for colonization (Butler & Camilli, 2004). Chemotaxis and motility greatly influence the infectivity of *V. cholerae*, but the role of chemotaxis genes in *V. cholerae* pathogenesis is poorly understood. Binding of a ligand causes a conformational change in methyl-accepting chemotaxis protein (MCP), which is sensed by the CheA–CheW complex and alters the activity of the protein kinase CheA (Falke *et al.*, 1997). CheA donates phosphate to two effectors, CheB and CheY. Phosphorylated CheY interacts with the flagellar motor protein FliM to influence the direction of flagellar rotation from counterclockwise to clockwise, reorienting the cell from a smooth swimming to a tumbling motion (Jones & Freter, 1976; Boin *et al.*, 2004).

The genome sequence of *V. cholerae* contains a large number of chemotaxis-related gene homologues (Heidelberg *et al.*, 2000) which are clustered in three different regions distributed on two chromosomes. In contrast to the single copy of CheY in *Escherichia coli* and *Salmonella typhimurium*, four CheYs (CheY1–CheY4) are present in the *V. cholerae* genome (Boin *et al.*, 2004). Pairwise sequence comparisons show that these CheYs share 30–39% identity and several studies have established that they are sufficiently different from each other and are not simply redundant versions of one CheY protein (Boin *et al.*, 2004). A comparative modelling and simulation study indicated that although the residues required for phosphorylation are conserved in all four CheYs, only CheY3 possesses the key structural elements required for FliM binding (Dasgupta & Dattagupta, 2008). Multiple copies of CheY (CheY1–CheY6) are also observed in *Rhodobacter sphaeroides* and studies are being carried

© 2011 International Union of Crystallography
All rights reserved

out to identify their role in FlIM binding (del Campo *et al.*, 2007; Porter *et al.*, 2006).

An attempt to identify the *V. cholerae cheY* gene responsible for flagellar motion showed that a deletion mutant of *cheY3* impairs chemotaxis (Butler & Camilli, 2004). An *in vivo* study also indicated that only CheY3 directly switches the flagellar rotation by interacting with FlIM (Hyakutake *et al.*, 2005). In contrast, another study indicated that while insertional disruption of the *cheY4* gene results in decreased motility, insertional duplication of this gene increases motility and is associated with enhanced expression of the two major virulence genes *ctxAB* and *tcpA*, suggesting a yet to be defined role of *cheY4* in the regulation of virulence factors (Banerjee *et al.*, 2002). A recent study indicates that *cheY3/cheY4* influence the activation of the transcription factor NF- κ B, an integral part of the signalling mechanism, to generate acute inflammatory responses (Bandyopadhyaya & Chaudhuri, 2009). However, the detailed mechanism of action of *cheY3/cheY4* is as yet unknown.

Considering the emerging importance of multiple copies of CheY in *V. cholerae*, especially of CheY4 and CheY3, we have taken the initiative to determine their structure in order to understand the molecular basis of their diverse functions. We have chosen *V. cholerae* strain O395 since it belongs to the widely investigated O1 serotype. Also, *V. cholerae* strain O395 CheY4 shows 98–100% sequence identity to those of other *Vibrio* strains, with practically no inter-

strain variation. The structure of CheY3 has been solved (unpublished work) and this study reports the cloning, overexpression, purification, crystallization and preliminary structure analysis of CheY4.

2. Materials and methods

2.1. Cloning, expression and purification of CheY4

CheY4 (UniProt accession No. A5F194) was primarily cloned in pGEM^T-Easy T/A cloning vector with ampicillin resistance using the forward primer 5'-CCCCGCATATGGCAAAGTTTGGCAGTAGATG-3' and the reverse primer 5'-GCCGGGATCCTTACAAAACGCGCTGCAAAG-3'. The primers were synthesized (NeuProCell) with *Nde*I and *Bam*HI restriction-enzyme sites. Chromosomal DNA of *V. cholerae* strain O395 was used as a template to amplify the region encoding *cheY4*. The *cheY4*-pGEM^T clone was double-digested with *Nde*I and *Bam*HI and the resulting 378 bp fragment was purified from 1.5% agarose gel. This fragment was then subcloned into pET28a⁽⁺⁾ vector (Novagen) for overexpression. The clones were selected appropriately using *E. coli* XL1-Blue cells with kanamycin resistance. CheY4 protein was then overexpressed (Fig. 1a) in *E. coli* BL21 (DE3) cells in the presence of kanamycin.

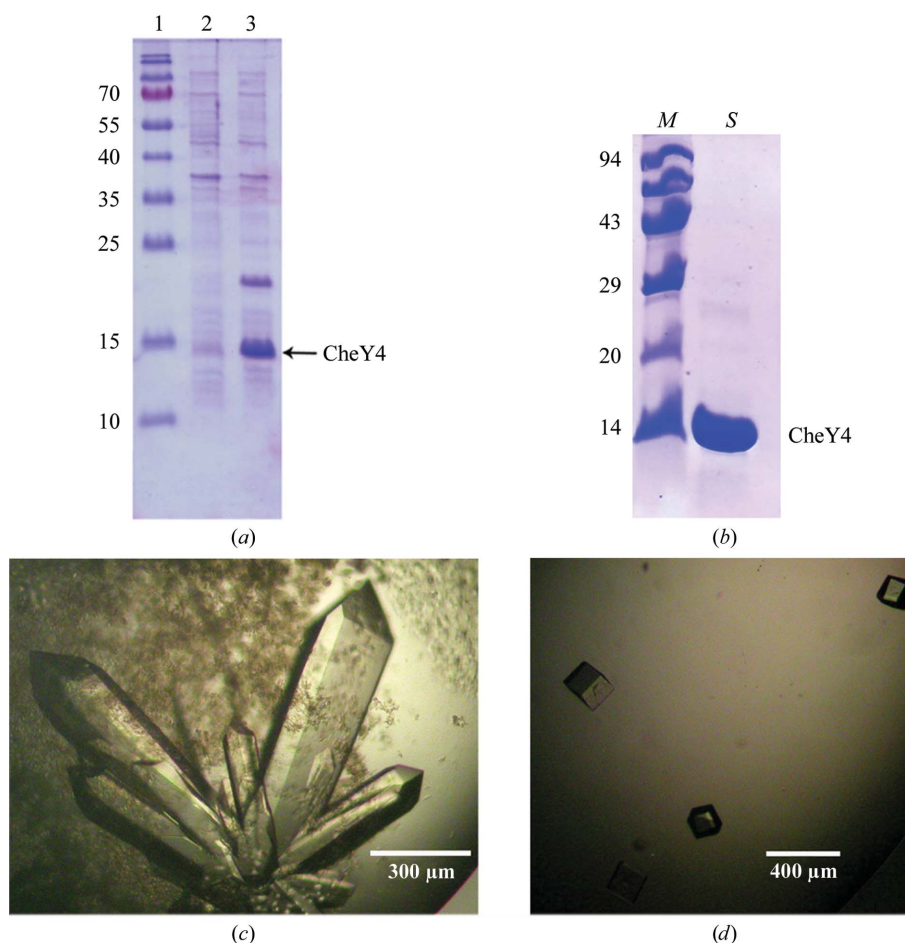


Figure 1
 (a) Overexpression of 6×His-tagged CheY4 showing uninduced and induced lanes (lanes 2 and 3, respectively) together with molecular-weight markers (lane 1; labelled in kDa) on 15% SDS-PAGE. (b) The homogeneity of the purified CheY4 was checked by 15% SDS-PAGE. CheY4 is shown in lane S; lane M contains molecular-weight markers (labelled in kDa). (c) Crystals of CheY4 grown in the presence of precipitant solution consisting of 0.8 M ammonium sulfate in 0.1 M Bicine and 4% glycerol at pH 9.0. (d) Crystals of CheY4 grown in precipitant solution consisting of 0.8 M ammonium sulfate in 0.1 M citrate and 4% glycerol at pH 4.0.

For overexpression, 1 l LB broth was inoculated with 10 ml overnight culture and the culture was grown at 310 K until the OD_{600} reached 0.6. The cells were then induced with 0.1 mM IPTG. After induction at 310 K for 3 h, the cells were harvested at 4500g for 20 min and the pellet was resuspended in 25 ml ice-cold lysis buffer containing 50 mM Tris-HCl pH 8.0 and 300 mM NaCl. PMSF (final concentration of 1 mM) and 10 mg lysozyme were added to the resuspended solution and it was lysed by sonication on ice. The cell lysate was then centrifuged (12 000g for 50 min) at 277 K and CheY4

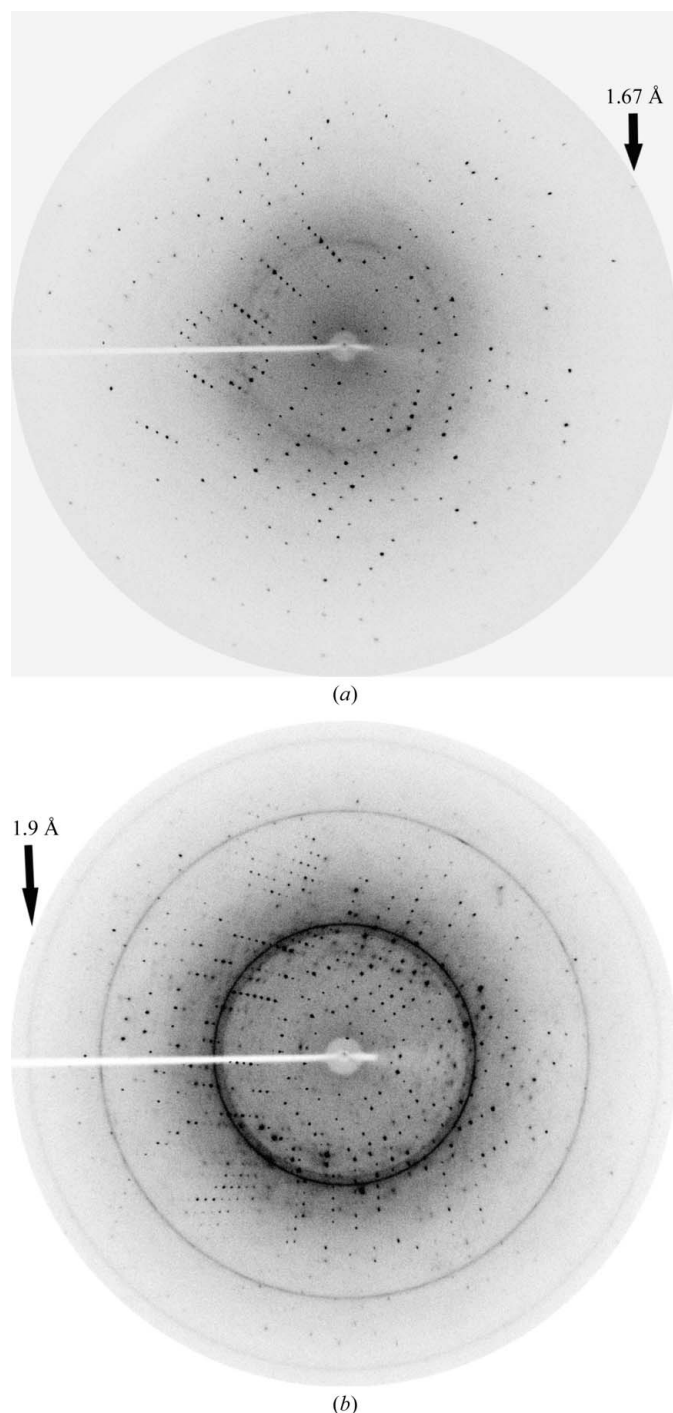


Figure 2
X-ray diffraction image of CheY4 crystals (a) grown under low-pH conditions and diffracting to a resolution of 1.67 Å and (b) grown under high-pH condition and diffracting to 1.9 Å resolution.

Table 1

Data-collection and data-processing parameters for CheY4 crystals.

Values in parentheses are for the outermost resolution shell.

Space group	C2	$P3_221$
Unit-cell parameters (Å, °)	$a = 94.4, b = 31.9,$ $c = 32.6, \alpha = 90,$ $\beta = 96.5, \gamma = 90$	$a = b = 56.104, c = 72.283,$ $\alpha = \beta = 90, \gamma = 120$
Oscillation range (°)	0.5	0.5
Resolution (Å)	30.0–1.67	30–1.9
No. of molecules per asymmetric unit	1	1
Mathews coefficient V_M (Å ³ Da ⁻¹)	1.88	2.33
Solvent content (%)	34	47
No. of observations	20715	44262
No. of unique reflections	11037	11181
Mosaicity (°)	0.3	0.25
Completeness (%)	95.3 (91.0)	92.0 (88.8)
R_{merge}^\dagger (%)	4.49 (10.05)	3.47 (22.44)
Average $I/\sigma(I)$	8.6 (3.0)	11.3 (2.0)

$^\dagger R_{\text{merge}} = \frac{\sum_{hkl} \sum_i |I_i(hkl) - \langle I(hkl) \rangle|}{\sum_{hkl} \sum_i I_i(hkl)}$, where $I_i(hkl)$ is the observed intensity of the i th measurement of reflection hkl and $\langle I(hkl) \rangle$ is the mean intensity of reflection hkl calculated after scaling.

with an N-terminal 6×His tag was isolated from the supernatant using Ni-NTA affinity chromatography (Qiagen). The 6×His-tagged CheY4 protein was eluted with lysis buffer containing 150 mM imidazole. The eluted fraction was checked by 15% SDS-PAGE and was found to be nearly homogeneous. The fractions were pooled, dialyzed overnight against thrombin cleavage buffer (0.1 M Tris-HCl pH 8.0, 150 mM NaCl) and concentrated using an Amicon ultra-centrifugation unit (molecular-weight cutoff 3000 Da), and the 6×His tag was cleaved with 1 U thrombin by overnight incubation at 277 K. This cloning process introduced a stretch of three non-native amino acids Gly-Ser-His before the N-terminus of the protein. The protein was further purified by gel filtration using a Sephacryl S-100 (GE Healthcare) column (78 × 1.4 cm) pre-equilibrated with thrombin cleavage buffer containing 0.02% sodium azide at 277 K. The homogeneity of the purified protein was checked by 15% SDS-PAGE (Fig. 1b).

2.2. Crystallization

CheY4 was concentrated to 9 mg ml⁻¹ (using a molar extinction coefficient ϵ_{280} of 8480 M⁻¹ cm⁻¹) in buffer consisting of 50 mM Tris-HCl pH 8.0, 150 mM NaCl for crystallization. Crystallization was performed by the hanging-drop vapour-diffusion method using 24-well crystallization trays (Hampton Research, Laguna Niguel, California, USA). Grid Screen Ammonium Sulfate, Crystal Screen and Crystal Screen 2 from Hampton Research (Jancarik & Kim, 1991) were used to explore the initial crystallization conditions. Initially, small crystals were obtained using ammonium sulfate as a precipitant at pH 4.0 and pH 9.0 at 293 K. Both of these crystallization conditions were further optimized and produced diffraction-quality crystals within a week. In the high-pH condition, hexagonal-shaped crystals (0.6 × 0.3 × 0.3 mm; Fig. 1c) were obtained from a drop consisting of 2 μl protein solution and an equal volume of precipitant (0.8 M ammonium sulfate, 0.1 M Bicine pH 9.0, 4% glycerol) equilibrated against 600 μl reservoir solution (1.6 M ammonium sulfate, 0.1 M Bicine pH 9.0, 2% glycerol). In the low-pH condition, cube-shaped crystals (0.2 × 0.2 × 0.2 mm; Fig. 1d) were obtained when 2 μl protein solution was mixed with an equal volume of precipitant (0.8 M ammonium sulfate, 0.1 M citrate, 4% glycerol) and equilibrated against 600 μl reservoir solution (2.4 M ammonium sulfate, 0.1 M citrate, 4% glycerol).

2.3. Data collection and processing

Crystals of CheY4 were picked out from the crystallization drops using a 10 μm nylon loop and flash-cooled in a stream of nitrogen (Oxford Cryosystems) at 100 K. Diffraction data sets were collected using an in-house MAR Research image-plate detector of diameter 345 mm and Cu $K\alpha$ radiation generated by a Bruker–Nonius FR591 rotating-anode generator equipped with Osmic MaxFlux confocal optics and operated at 50 kV and 70 mA. Data were processed and scaled using *automar* (<http://www.marresearch.com/automar/run.html>). Data-collection and processing statistics are given in Table 1.

3. Results

CheY4 was overexpressed as a 6 \times His-tagged protein (Fig. 1*a*) and purified by Ni–NTA affinity chromatography. The 6 \times His tag was cleaved by thrombin and the protein was further purified by gel filtration and concentrated to 9 mg ml⁻¹ (Fig. 1*b*) for crystallization. Crystals grown under low-pH conditions (Fig. 1*d*) belonged to space group *C2*, with unit-cell parameters $a = 94.4$, $b = 31.9$, $c = 32.6$ Å, $\beta = 96.5^\circ$, and diffracted to 1.67 Å resolution (Fig. 2*a*). Crystals grown under high-pH conditions (Fig. 1*c*) belonged to space group *P3₂21*, with unit-cell parameters $a = b = 56.104$, $c = 72.283$ Å, $\gamma = 120^\circ$, and diffracted to 1.9 Å resolution (Fig. 2*b*). Packing considerations based on the molecular weight of 13.2 kDa indicated the presence of one molecule in the asymmetric unit in both cases, corresponding to Matthews coefficients V_M (Matthews, 1968) of 1.88 and 2.33 Å³ Da⁻¹ for space groups *C2* and *P3₂21*, respectively. The corresponding solvent-content values are 34 and 47%, respectively.

A *BLAST* (Altschul *et al.*, 1990) search with the *V. cholerae* CheY4 sequence against the PDB showed that CheY from *S. typhimurium* (PDB entry 2che; Stock *et al.*, 1993) gives the highest score, with 41% identity. The coordinates of the Mg²⁺-bound structure of *S. typhimurium* CheY (PDB entry 2che) was therefore retrieved and its polyalanine model was used in molecular-replacement (MR) calculations for the monoclinic data set. However, this model did not produce a convincing solution. A polyalanine model prepared from the structure of *V. cholerae* CheY3 (which has only 36% sequence identity to *V. cholerae* CheY4), which was solved recently in our laboratory (unpublished results), yielded a better solution. One molecule of this polyalanine model in the asymmetric unit produced a correlation coefficient of only 34.6% with an *R* factor of 49.3% using data in the resolution range 10–4.5 Å. Rigid-body refinement followed by a few cycles of positional refinement by *CNS* (Brünger *et al.*, 1998) using data in the resolution range 10–2.8 Å produced an *R* factor of 43.5% ($R_{\text{free}} = 46.2\%$). The electron density was continuous

except for helix $\alpha 4$. One cycle of model fitting and incorporation of highly conserved side chains, wherever electron density permitted, yielded an *R* factor of 38.4% ($R_{\text{free}} = 42.1\%$). This structure was then used directly as a search model for the data set in space group *P3₂21* and produced an unambiguous solution with a correlation coefficient of 52.6% and an *R* factor of 42.3% using data in the resolution range 10–4.0 Å. All molecular-replacement calculations were performed using *MOLREP* from the *CCP4* package (Winn *et al.*, 2011) and model fitting was performed using *O* (Jones *et al.*, 1991). Further refinement and model building is in progress.

JD is grateful to Dr Felix Raj SJ, Principal, St Xavier's College, Kolkata for his encouragement and constant support. JD and MB are grateful to the members of the crystallography laboratory at SINP for their support. This work was supported by the Council of Scientific and Industrial Research [grant No. 37(1381)/09/EMR-II], Government of India.

References

- Altschul, S. F., Gish, W., Miller, W., Myers, E. W. & Lipman, D. J. (1990). *J. Mol. Biol.* **215**, 403–410.
- Bandyopadhyaya, A. & Chaudhuri, K. (2009). *Innate Immun.* **15**, 131–142.
- Banerjee, R., Das, S., Mukhopadhyay, K., Nag, S., Chakraborty, A. & Chaudhuri, K. (2002). *FEBS Lett.* **532**, 221–226.
- Boin, M. A., Austin, M. J. & Häse, C. C. (2004). *FEMS Microbiol. Lett.* **239**, 1–8.
- Brünger, A. T., Adams, P. D., Clore, G. M., DeLano, W. L., Gros, P., Grosse-Kunstleve, R. W., Jiang, J.-S., Kuszewski, J., Nilges, M., Pannu, N. S., Read, R. J., Rice, L. M., Simonson, T. & Warren, G. L. (1998). *Acta Cryst.* **D54**, 905–921.
- Butler, S. M. & Camilli, A. (2004). *Proc. Natl Acad. Sci. USA*, **101**, 5018–5023.
- Campo, A. M. del, Ballado, T., de la Mora, J., Poggio, S., Camarena, L. & Dreyfus, G. (2007). *J. Bacteriol.* **189**, 8397–8401.
- Dasgupta, J. & Dattagupta, J. K. (2008). *J. Biomol. Struct. Dyn.* **25**, 495–503.
- Falke, J. J., Bass, R. B., Butler, S. L., Chervitz, S. A. & Danielson, M. A. (1997). *Annu. Rev. Cell Dev. Biol.* **13**, 457–512.
- Heidelberg, J. F. *et al.* (2000). *Nature (London)*, **406**, 477–483.
- Hyakutake, A., Homma, M., Austin, M. J., Boin, M. A., Häse, C. C. & Kawagishi, I. (2005). *J. Bacteriol.* **187**, 8403–8410.
- Jancarik, J. & Kim, S.-H. (1991). *J. Appl. Cryst.* **24**, 409–411.
- Jones, G. W. & Freter, R. (1976). *Infect. Immun.* **14**, 240–245.
- Jones, T. A., Zou, J.-Y., Cowan, S. W. & Kjeldgaard, M. (1991). *Acta Cryst.* **A47**, 110–119.
- Matthews, B. W. (1968). *J. Mol. Biol.* **33**, 491–497.
- Porter, S. L., Wadhams, G. H., Martin, A. C., Byles, E. D., Lancaster, D. E. & Armitage, J. P. (2006). *J. Biol. Chem.* **281**, 32694–32704.
- Stock, A. M., Martinez-Hackert, E., Rasmussen, B. F., West, A. H., Stock, J. B., Ringe, D. & Petsko, G. A. (1993). *Biochemistry*, **32**, 13375–13380.
- Winn, M. D. *et al.* (2011). *Acta Cryst.* **D67**, 235–242.